JOURNAL OF MATERIALS SCIENCE 26 (1991) 6260–6270

Fracture at bimaterial interfaces: the role of residual stresses

A. J. KINLOCH, E. THRUSABANJONG, J. G. WILLIAMS
Imperial College of Science, Technology and Medicine, Department of Mechanical Engineering, Exhibition Road, London SW7 2BX, UK

Crack growth along a bimaterial interface consisting of an epoxy adhesive bonded to an aluminium alloy substrate has been studied. The results have been analysed using the concepts of linear elastic fracture mechanics and the fracture energies associated with the various failure modes have been deduced. It is demonstrated that residual stresses present in a symmetrical bimaterial joint have a major influence upon both the locus of joint failure and the measured fracture energy.

1. Introduction

Adhesively, bonded joints have become increasingly popular in engineering applications and the structural integrity of such components has, therefore, become an important design aspect. The use of continuum fracture mechanics is an established method for the assessment of the service lifetime of homogeneous materials and structures, and has been applied to the design and the prediction of service life of adhesive joints [1].

The application of fracture mechanics to the cohesive fracture of adhesively bonded joints is somewhat more complex than that of homogeneous materials [1–3]. However, the most severe problems are encountered when interfacial failure needs to be considered [4–9]. Indeed, crack growth along the adhesive/substrate interface is of major importance, and environmental attack upon adhesive joints [10] is an example where such failure frequently occurs.

The present paper is concerned with the failure of adhesive joints which are modelled as a bimaterial interface consisting of an epoxy adhesive bonded to an aluminium alloy substrate. The paper concentrates upon the effects of residual stresses which are present when the adhesive is post-cured. Indeed, it is shown that only when such stresses are present is interfacial failure observed in the present joints (which are tested in a benign environment) and that the contribution of such stresses to the failure process must be considered.

2. Theoretical aspects

2.1. Introduction

From using the concepts of fracture mechanics two main, inter-relatable, conditions for fracture are proposed. Firstly, the energy criterion arising from Griffith's [11], and later Orowan's [12], work which supposes that fracture occurs when sufficient energy is released (from the stress field) by growth of the crack to supply the energy requirements of the new fracture surfaces. The energy released comes from stored elastic or potential energy of the loading system and can, in principle, be calculated for any type of test piece. This approach, therefore, provides a measure of the energy required to extend a crack over unit area and this is termed the fracture energy or critical strain energy release rate and is often denoted by G_c. Secondly, Irwin [13] found that the stress field around a sharp crack in a linear elastic material could be uniquely defined by a parameter named the stress intensity factor, K, and stated that fracture occurs when the value of K exceeds some critical value, K_c. Thus K is a stress-field parameter independent of the material whereas K_c, often referred to as the fracture toughness, is a measure of a material property. A basic aim of fracture mechanics is to identify fracture criteria such as G_c and K_c which are independent of the geometry of the cracked body.

2.2. Bulk (homogeneous) materials

For a sharp crack in a uniformly stressed, infinite, homogeneous lamina and, assuming Hookean behaviour and infinitesimal strains, i.e. linear elastic fracture mechanics (LEFM), Westergaard [14] has developed certain stress functions which relate the local stress concentration of stresses at the crack tip to the applied stress, σ_0. For regions close to the crack tip the solutions take the form

$$\sigma_{ij} = \sigma_0 \left(\frac{a}{2r}\right)^{1/2} f_{ij}(\theta) \qquad (1)$$

where σ_{ij} are the components of the stress tensor at a point, r and θ are the polar coordinates of the point, taking the crack tip as the origin, and $2a$ is the length of the crack.

Irwin [13] modified this solution to give

$$\sigma_{ij} = \frac{K}{(2\pi r)^{1/2}} f_{ij}(\theta) \qquad (2)$$

The parameter K is the stress intensity factor and relates the magnitude of the stress intensity local to

0022-2461/91 $03.00 + .12 © 1991 Chapman & Hall

the crack in terms of the applied loadings and geometry of the structure in which the crack is located. A crack may be stressed in three different modes, denoted I, II and III. The cleavage or tensile-opening mode, Mode I, is the most commonly encountered and usually the one which most often results in failure. However, if the crack is constrained, as may be the case in adhesive joints or polymeric-fibre composites, attention must sometimes be given to Modes II (in-plane shear) and III (anti-plane shear).

The power of this approach is that the stress intensity factor, K_c, at crack growth may be expressed by an equation of the form

$$K_{Ic} = Y\sigma_c a^{1/2} \quad (3)$$

where K_{Ic} is the Mode I fracture toughness, σ_c is the applied stress at the onset of crack growth and Y is a geometry constant. For the single-edge notch specimen loaded in tension, the value of Y is given [15] by

$$Y = 1.99 - 0.41\left(\frac{a}{W}\right) + 18.70\left(\frac{a}{W}\right)^2 - 38.48\left(\frac{a}{W}\right)^3 + 53.85\left(\frac{a}{W}\right)^4 \quad (4)$$

where W is the width of the crack.

Considering the energy balance approach, and assuming that the material behaves in a linear elastic manner (i.e. that linear elastic fracture mechanics is applicable) then the fracture energy, G_{Ic}, is given by

$$G_{Ic} = \frac{P_c^2}{2}\frac{dC}{da} \quad (5)$$

where P_c is the load for the onset of crack growth per unit thickness and C is the compliance of the specimen, given by $C = \delta/P$ where δ is the displacement.

In the case of a bulk material, the relationship between K and G is given, for plane-strain conditions, by

$$K^2 = \frac{EG}{1 - \nu^2} \quad (6)$$

where ν is the Poisson's ratio.

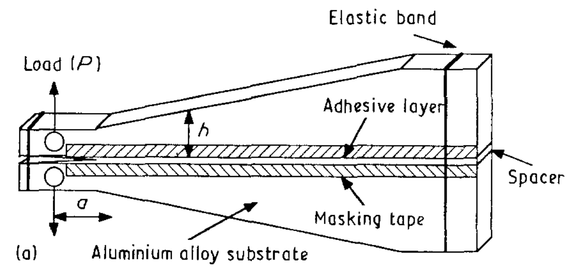

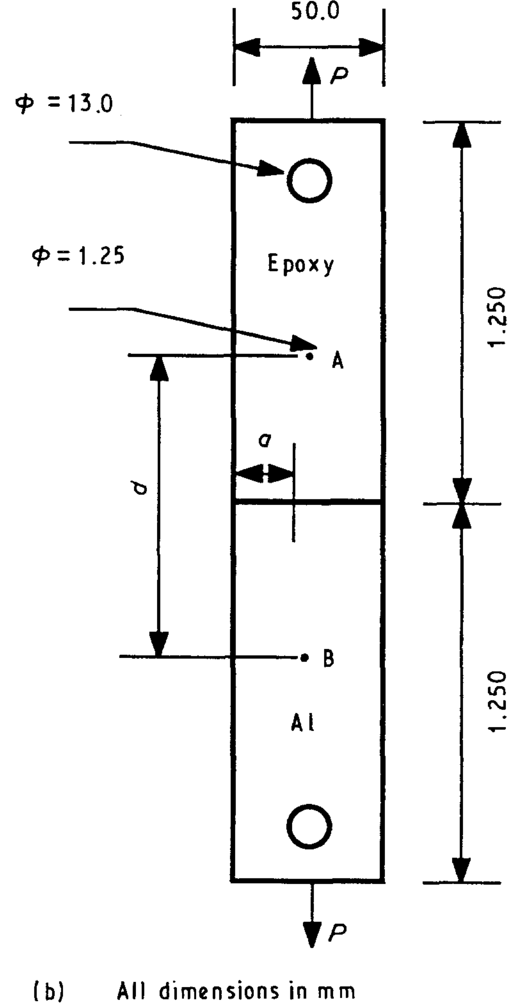

Figure 1 (a) Tapered double cantilever beam (TDCB) joint specimen. (b) Symmetrical bimaterial (SBM) joint specimen.

2.3. Bimaterial interfaces

Considering firstly the stress intensity factor approach, then an immediate problem arises when a crack is at a bimaterial interface. Namely, when the joint is subjected solely to tensile loads applied normal to the interfacial crack (see Fig. 1b), these tensile loads will induce both tensile and shear stresses around the crack tip. Therefore, both K_{Ii} and K_{IIi} terms are needed; the subscript "i" indicating a crack the interface. However, these K_{Ii} and K_{IIi} terms no longer have the clearly defined physical significance, as for the bulk (homogeneous) material case discussed above. Mathematical modelling has shown [4–9] that, for linear elastic materials, the local stresses ahead of the crack tip at a bimaterial interface are proportional to

$$\frac{f(K_{Ii}, K_{IIi})}{(2\pi r)^{1/2}}\left(\frac{\sin}{\cos}\right)(\xi \ln r) \quad (7)$$

where ξ is a "bimaterial constant" and is a function of the moduli and Poisson's ratios of the two materials forming the interface. Thus, it may be seen from Equation 6 that the singular behaviour of the stresses is again proportional to the inverse square of the distance, r. But unlike the bulk material case, a major consequence of the above relationship is that very close to the crack tip the stresses are oscillatory and have the highly improbable property of changing signs with increasing frequency as $r \to 0$. Even more unlikely, the crack face displacements also oscillate and impinge, and near the crack tip interfere, giving a physically impossible solution. A further complication is that the analysis results in a logarithmic term of a dimensional parameter, r. Thus, the crack-tip stresses, and values of K, become a function of the measuring units of r. Various modifications have been suggested to overcome the above difficulties but many

workers have chosen to adopt the energy balance approach to avoid the inherent problems associated with the stress intensity factor.

For LEFM, the value of the adhesive fracture energy, for either a cohesive crack or an interfacial crack (denoted by G_a or G_{ic}, respectively), may be explicitly expressed by

$$G_a \text{ or } G_{ic} = \frac{P_c^2}{2}\frac{dC}{da} \quad (8)$$

The value of dC/da may either be estimated theoretically (numerically or analytically) or experimentally. In the course of the present work all these various methods are adopted. Often it is convenient to normalize the crack length with respect to the width, W, hence

$$G_a \text{ or } G_{ic} = \frac{P_c^2}{2W}\frac{dC}{d(a/W)} \quad (9)$$

In the case of the tapered double cantilever beam joint (see Fig. 1a) using metallic isotropic substrates the rate of change of compliance with crack length, dC/da, is given, for unit thickness, from beam theory by [16–18]:

$$\frac{dC}{da} = \frac{8}{E_s}\left(\frac{3a^2}{h^3} + \frac{1}{h}\right) \quad (10)$$

where E_s is the modulus of the substrate beam and h is the height of the beam at a crack length a.

2.4. Boundary integral equation (BIE) method

The boundary integral equation (BIE) method was used in the present work for the numerical calculations of the compliance of the SBM specimens, the evaluation of the stresses along the interface induced by differential thermal contraction and the associated energy release rate. The computer program used has been previously described [19, 20] and the smallest element used in the mesh was 10^{-5} of the relevant crack length.

3. Experimental procedure

3.1. Materials

The epoxy adhesive employed was the diglycidyl ether of bisphenol A resin cured with triethylene tetramine hardener in the proportions of 100 parts of resin to 10 parts of hardener by weight. The two parts were mixed thoroughly at room temperature and then the air was removed by placing the mixture in a vacuum oven at 20 °C for 30 min. This adhesive system was selected as it could be cured at room temperature and then post-cured at various temperatures. Also, it was a relatively brittle material and therefore enabled LEFM theory to be applied.

The substrate was aluminium alloy (BS 1470:H30-TF) and the surface to be bonded was subjected to a treatment of grit-blasting, using 180–220 mesh alumina, followed by degreasing in a liquid, and then a vapour, bath of 1, 1, 1 trichloroethane. The cure schedule employed was to first cure the adhesive for 24 h at 20 °C. This was followed by a post-curing operation. The post-cure conditions used were one of the followng: (i) 6 days at 20 °C; (ii) 2 days at 45 °C; (iii) 2 days at 80 °C; (iv) 2 days at 120 °C, or (v) 2 days at 150 °C. For all the elevated cure conditions the specimens were allowed to cool slowly in the oven. All fracture tests were conducted at a constant rate of displacement of 0.5 mm min^{-1} and at 20 °C.

3.2. Bulk fracture studies

To ascertain the bulk values of G_{Ic} and K_{Ic} the test geometry used was the single-edge notched (SEN) specimen. Cracks were introduced into the specimen by the usual manner of tapping a razor blade into the edge and ensuring that a natural (sharp) crack grew ahead of the blade. The pre-cracked specimens were then subjected to applied tensile loads and the fracture stress ascertained as a function of crack length.

3.3. Joint fracture studies

3.3.1. Tapered double cantilever beam (TDCB) specimens

The TDCB joint specimens are shown schematically in Fig. 1a. To prepare these test specimens, one side of each of the two substrate beams was first masked with tape, which was removed after the adhesive had hardened. This was done in order to prevent any adhesive which leaked from the adhesive layer adhering to the sides of the beams. On the other side of the beams the masking tape was placed across a gap maintained between the beams; this gap being controlled by two small 0.5 mm thick plastic spacers which were inserted into either end of the joint. Elastic bands were placed around the beams to hold them firmly together. This (sealed) side of the joint was placed down on to the bench and adhesive poured into the gap. To form a cohesive starter crack a piece of aluminium foil, which had been previously coated with release agent, was inserted into the liquid adhesive which was now filling the gap between the two metal substrate beams. The elastic bands and masking tape were removed after the epoxy adhesive had been allowed to harden for 24 h at 20 °C. Upon testing, the loads for crack growth were only recorded after a natural crack had been allowed to propagate ahead of the aluminium foil.

3.3.2. Symmetrical bimaterial (SBM) specimens

The SBM specimen is shown schematically in Fig. 1b. This was prepared by casting the epoxy adhesive directly on to the aluminium alloy substrate. Prior to the casting operation the substrate was cleaned as described above and an "incipient" interfacial starter crack inserted. The interfacial starter cracks were inserted at the epoxy/substrate interface by painting the cleaned surfaces along part of their length with a release agent (Ciba Geigy "QZ13") which had been diluted with acetone in the ratio of 1 to 2 by volume. This method ensured a sharper crack than either polytetrafluoroethylene tape or polyethylene sheet, because the release agent gave a very thin layer and

TABLE I Values of K_{Ic}, E and G_{Ic} for the bulk epoxy materials as a function of the post-cure temperature employed

Post-cure temp. (°C)	Tensile modulus, E (GPa)	K_{Ic} (MPa m$^{1/2}$)	G_{Ic} (J m^{-2})	T_g (°C)	Coeff. thermal exp, α (linear °C^{-1})
20	3.47	0.53	69.8	48	37.1×10^{-6}
45	3.86	0.65	96.7	65	43.6×10^{-6}
80	3.29	0.53	71.8	102	44.7×10^{-6}
120	2.57	0.68	157.6	134	51.0×10^{-6}
150	2.61	0.94	296.3	123	54.4×10^{-6}

Note: α for aluminium alloy = 23.0×10^{-6} linear °C^{-1}.

hence a very sharp crack tip. The casting was undertaken using a silicone rubber mould. The mould was first coated with release agent and the aluminium alloy was then placed in the mould. Next the adhesive mixture was poured into the mould, via a filler hole until adhesive appeared at the vent-hole. The SBM joint was then subjected to 24 h at 20 °C and then removed from the mould. The joint was then post-cured using one of the various post-cure conditions listed above.

4. Results and discussion

4.1. Bulk fracture studies

The stress intensity factor, K_{Ic}, at the onset of crack growth was determined for the bulk epoxy materials using the single-edge notched (SEN) test specimen, as described above. Sharp cracks were inserted using a razor-blade and, upon loading at a constant displacement rate, this crack propagated in an unstable manner through the SEN specimen. The stress at fracture was recorded and, from Equation 3, $Y^2\sigma_c^2$ was plotted against the reciprocal of the crack length, a^{-1}. Typical plots are shown in Fig. 2 for three different post-cure temperatures. As may be seen, good linear relationships are obtained and the slope of these relations yields the respective value of K_{Ic}. The tensile moduli, E, of the various materials were measured using dumb-bell shaped specimens and the values of E were used in Equation 6 to enable the corresponding values of the fracture energy, G_{Ic}, to be deduced. Values of K_{Ic}, E and G_{Ic} are shown in Table I. Also shown are values of the glass transition temperature, T_g, and the linear coefficient of thermal expansion of the epoxy polymers. The values of K_{Ic}, E and G_{Ic} reveal an initial rise in modulus and toughness when a post-cure temperature of 45 °C is employed. Upon the use of higher post-cure temperatures, the modulus declines and the toughness initially falls and then recovers. This type of complex behaviour has been previously observed [21, 22] and has been suggested to arise from the formation of inhomogeneous network structures in the epoxy polymer.

4.2. Tapered double cantilever beam joints

The compliance calibration was experimentally determined for the tapered double cantilever beam (TDCB) joints and is shown in Fig. 3. The values of the adhesive fracture energy, G_a, for joints containing an initial cohesive starter crack were evaluated using the tapered double cantilever beam joint specimen shown in Fig. 1a. Crack growth occurred by cohesive crack propagation through the adhesive layer in an unstable (i.e. stick–slip) manner. The initiation values of G_a were calculated from Equations 9 and 10 and are given in Table II. As may be seen, the values of G_a from the TDCB joint specimens where cohesive crack growth occurs are in excellent agreement with the values of G_{Ic} from the bulk fracture studies discussed above. This is in accord with previous studies [3] which have demonstrated that when the plastic-zone size is significantly smaller than the thickness of the adhesive layer, as in the case of the brittle epoxy polymers used in the present studies, the value of G_a is equivalent to G_{Ic}.

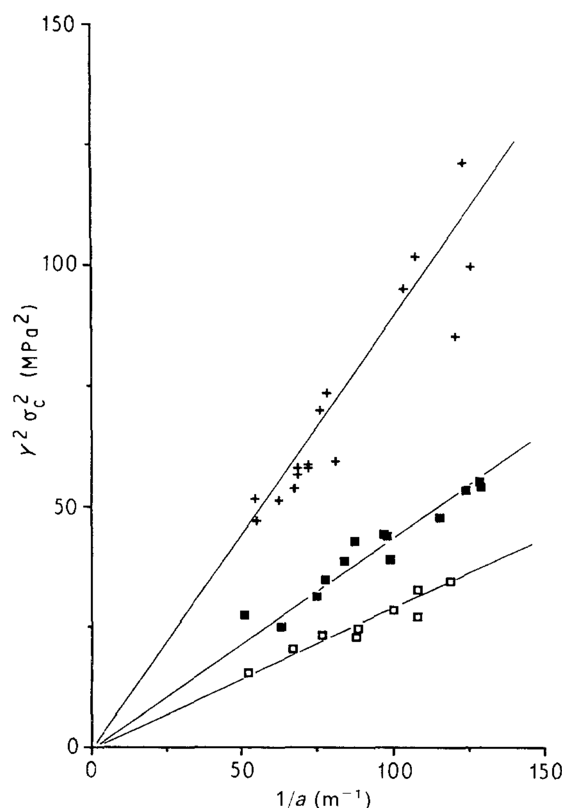

Figure 2 Plots based upon Equation 3 to determine K_{Ic} values from using the single-edge notched (SEN) bulk epoxy specimens. Results from three post-cure temperatures are shown. (□) 20 °C, (■) 45 °C, (+) 150 °C.

TABLE II Values of the fracture energies from the various test specimens employed

Post-cure temp. (°C)	SBM			TDCB	Bulk SEN
	G_{ic} ($J m^{-2}$)	G_{eff} ($J m^{-2}$)	G'_{eff} ($J m^{-2}$)	G_a ($J m^{-2}$)	G_{Ic} ($J m^{-2}$)
20	64.9+	–	–	64.8+	69.8+
45	22.3*	32.2*	61.7*	80.4+	96.7+
80	4.9*	33.0*	56.4*	71.7+	71.8+
120	5.8*	107.1*	155.6*	162.0+	157.6+
150	24.9*	250.0*	399.4*	285.3+	296.3+

Notes:
(a) G_{ic} values are the measured values for an adhesive joint with an interfacial starter crack.
(b) G_a values are for an adhesive joint with a cohesive starter crack.
(c) G_{eff} values are calculated from the G_{ic} values but allow for the contribution from elastic residual thermal stresses in the joints by summing energies.
(d) G'_{eff} values are calculated from the G_{ic} values but allow for the contribution from elastic residual thermal stresses in the joints by summing stresses.
(e) G_{Ic} values are for bulk epoxy (adhesive) specimens.
(f) Values marked * are for interfacial crack propagation.
(g) Values marked + are for cohesive crack propagation in the epoxy adhesive.

4.3. Symmetrical bimaterial (SBM) joint specimen

4.3.1. Compliance measurements

The compliance of the symmetrical bimaterial (SBM) joint specimens subjected to applied tensile loads was measured as described earlier and is shown as a function of the non-dimensionalized crack length, a/W, in Fig. 4 for post-cure temperatures of 20 and 45 °C. Also, shown are the theoretical results from the boundary integral equation (BIE) method, and good agreement exists between experiment and theory. Fig. 5 plots the differential of compliance with respect to crack length, $dC/d(a/W)$, versus a/W for three different specimens: a homogeneous epoxy sheet, a homogeneous aluminium sheet and an SBM joint. Again, both experimental and theoretical results are shown and the agreement is excellent. This obviously gives confidence in the numerical BIE analyses.

4.3.2. Fracture studies

The adhesive fracture energy, G_{ic}, for the SBM joint specimens may be calculated from Equation 8 or 9. In the case of the specimens where a post-cure temperature of 20 °C was employed, the data are plotted

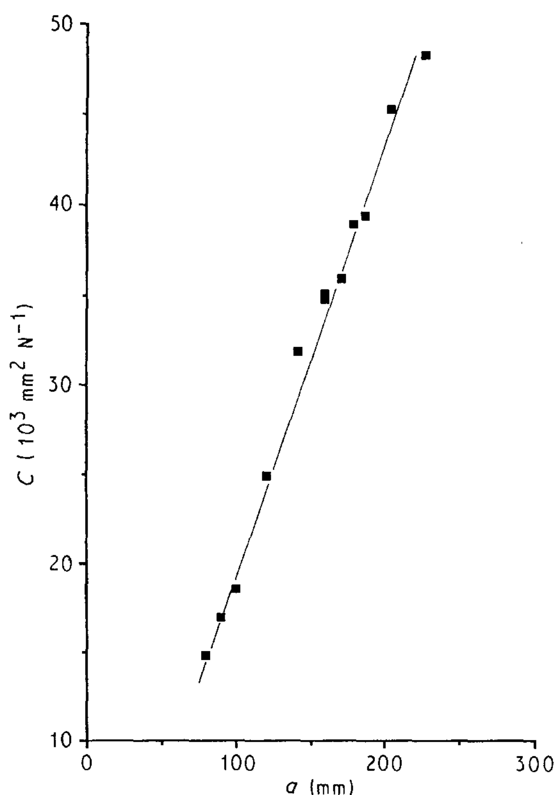

Figure 3 Compliance of the TDCB joint specimen as a function of crack length.

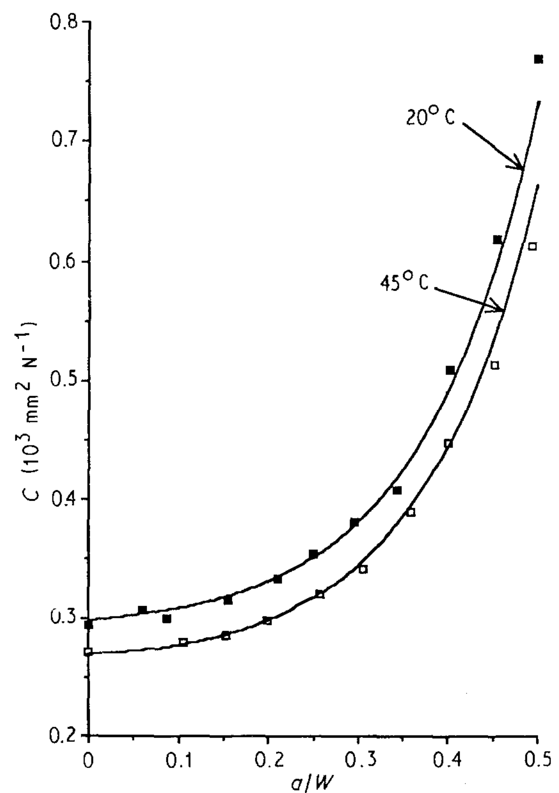

Figure 4 Compliance of the SBM joint specimen as a function of normalized crack length, a/W, from both (□, ■) experimental and (——) theoretical studies for post-curing temperatures of (■) 20 and (□) 45 °C.

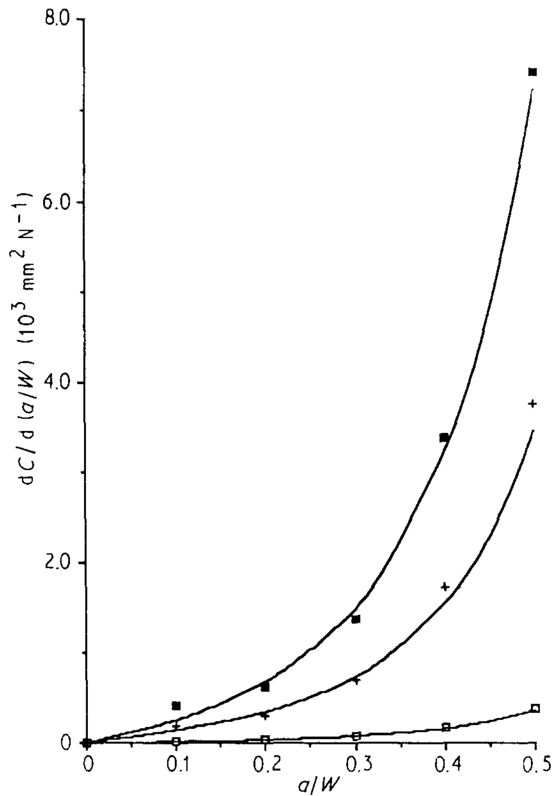

Figure 5 Rate of change of compliance with normalized crack length as a function of crack length for (+) SBM joint specimens and for (■) bulk epoxy and (□) aluminium alloy specimens. Results from (■, □, +) experimental and (——) theoretical studies are shown.

according to Equation 9 in Fig. 6a and an excellent linear fit, passing through the origin is obtained. As described below, in these joints the initial interfacial crack immediately diverted into the adhesive layer and the value of the fracture energy represents that for cohesive failure of the adhesive layer. For the higher post-cure temperatures reasonable linear relationships are also obtained, as shown in Fig. 6b. However, when individual values of G_{ic} are calculated and plotted as a function of a/W (see Fig. 6c), there does appear to be a significant trend of G_{ic} increasing with increasing length of the initial crack. This obviously invalidates an LEFM approach, and will be discussed in detail in Section 4.3.5. The average value of the fracture energy, from obtaining the best linear fit to the data shown in Fig. 6b, is given in Table II.

There are several points to consider from the data shown in Table II. Firstly, in the case of the SBM joints which were only subjected to a post-cure temperature of 20 °C the interfacial starter crack did not propagate along the epoxy/aluminium interface but immediately diverted into the epoxy layer. Thus, joint failure was via cohesive fracture of the epoxy layer. The value of G_{ic} recorded is in good agreement with the values of G_a and G_{Ic}, where these latter values also correspond to cohesive fracture through the epoxy adhesive. For the SBM specimens post-cured at 45, 80, 120 and 150 °C then the original interfacial starter crack did initially propagate along the interface and the average values of G_{ic} for interfacial failure from plots such as that shown in Fig. 6b are quoted in Table II. However, after propagating along the interface for some distance the crack suddenly diverted into the adhesive layer and, thus, the final phase of joint fracture was via cohesive failure in the adhesive. The higher the post-cure temperature then the longer was the distance of interfacial crack growth prior to the crack diverting into the adhesive layer. It was only possible to calculate the fracture energy at which cohesive failure was observed for the 45 °C SBM specimen and the value was 89.7 J m^{-2}, in reasonable agreement with the values of G_a and G_{Ic} of 80.4 and 96.9 J m^{-2}, respectively, for cohesive failure through the adhesive layer for this post-cure temperature. These observations would indicate that the post-cure temperature is affecting the locus of crack growth, which suggests that the residual stresses induced by the post curing may be of importance.

Secondly, whilst the values for cohesive fracture through the adhesive layer are in reasonable agreement with the values from the bulk SEN and TDCB specimens, the average values of G_{ic} for interfacial failure in the SBM specimens (marked * in Table II) are very low indeed. This again suggests the possible role of the residual stresses induced by the post-curing operation.

4.3.3. Residual stresses

The presence of residual stresses in structures can significantly influence their fracture behaviour. In adhesive bonding of two different materials residual stresses may arise (i) as a result of differential contraction between the materials when they are cooled from a higher temperature due to the different coefficients of thermal expansion of the materials, and (ii) from a volume contraction which often accompanies curing, or cross-linking, of the adhesive. The epoxy materials used in the present study were transparent and possessed photoelastic properties and, therefore, the extent of residual stresses could be observed using photoelasticity. A circular polariscope was employed whereby the isochromatic fringe patterns could be examined under white light, except for the specimens cured at the highest curing temperature of 150 °C when a plane polariscope was employed. The extent of the overall residual stress in the epoxy adhesive forming an SBM joint was recorded by photographing the fringe patterns through the polariscope.

The results for the "as-post-cured" SBM joints are shown in the left-hand column of Fig. 7 for the case where the initial interfacial crack length, a, was 10 mm. Results from using post-cure temperatures of 45, 80, 120 and 150 °C are given, no distinct fringe pattern being seen in the adhesive layer when the SBM joints were post-cured at room temperature. The photographs on the left-hand side of Fig. 7 clearly show an increase in the number of fringes as the post-cure temperature is increased, revealing that the extent of overall residual stress in the adhesive layer increases with increasing post-cure temperature as expected. The areas of high stress concentration such as the crack tip and the edge of the bond can also be easily identified from the fringe patterns.

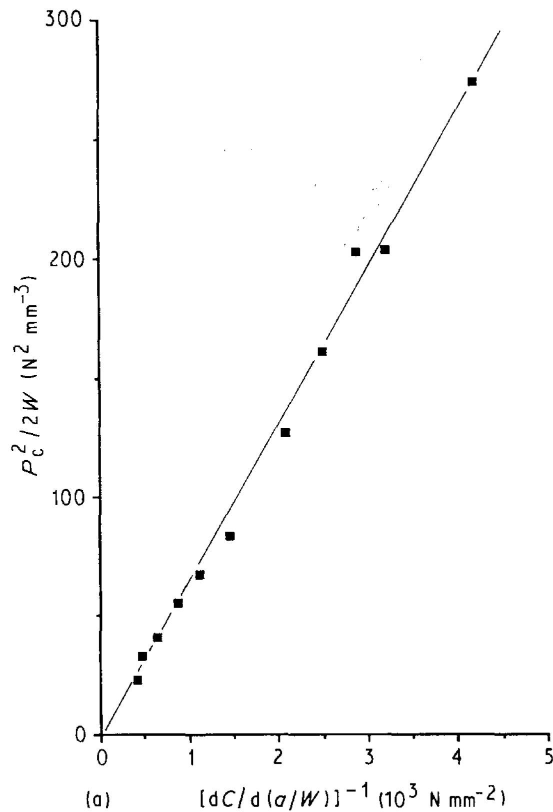

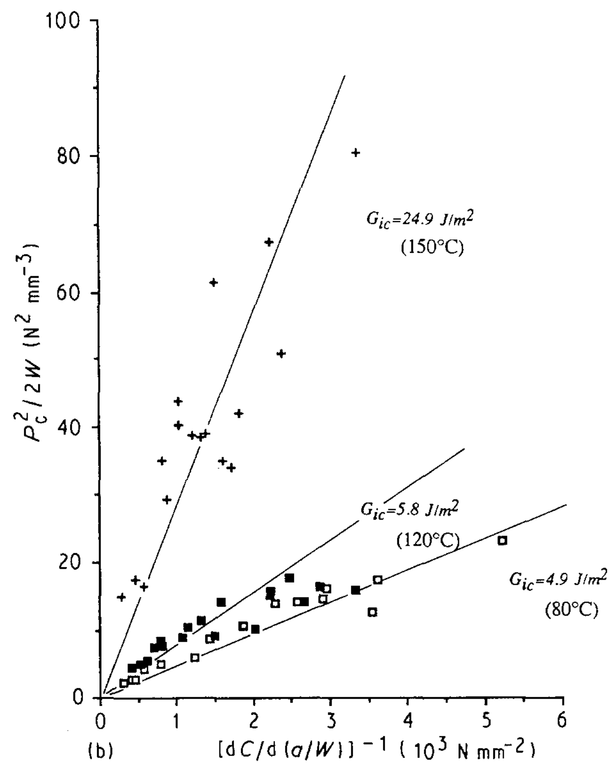

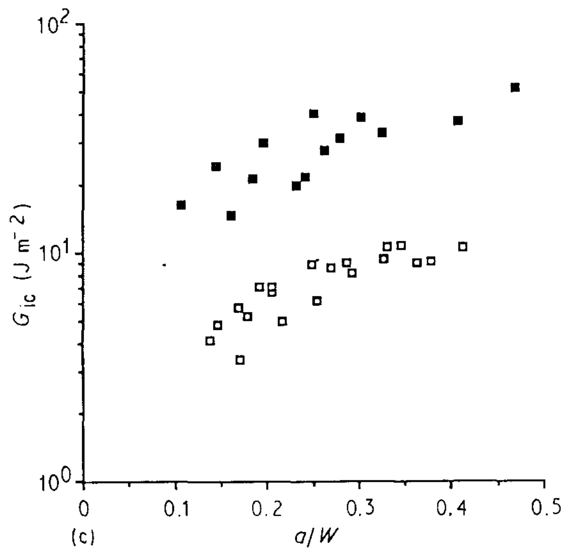

Figure 6 (a, b) Plots based upon Equation 9 to determine G_{ic} values from using the SBM joint specimen (a) A post-cure temperature of 20 °C has been used. (b) Post-cure temperatures of (□) 80, (■) 120 and (+) 150 °C have been used. (c) G_{ic} as a function of normalized crack length, a/W, from the SBM joint specimens for post-cure temperatures of (□) 120 and (■) 150 °C.

The next experiment which was conducted was to fracture the SBM joint along the adhesive/aluminium interface and then to re-examine the sheet of epoxy adhesive which had been freed from the aluminium alloy substrate in this manner. This was done in order to investigate whether the residual stresses observed above were fully released upon "removal" of the constraining metal substrate. To achieve this, the approach of Mulville and Vaishnav [23] was followed and a compressive force was applied along the edges of the substrate. Upon applying such a compressive force, it was found that, whilst the initial interfacial crack propagated slowly along the interface, a new interfacial crack developed at the other end of the interface and the two cracks eventually met somewhere in the central region of the interface. The epoxy adhesive layer was then re-examined in the polariscope and the resulting photographs are shown in the right-hand column of Fig. 7. As may be seen, the number of fringes for any given post-cure temperature has greatly decreased but there is a fringe pattern still remaining after debonding of the adhesive layer from the metal substrate.

This result is reasonable because the original residual stress pattern was established with the crack present and gave a rather complicated distribution, particularly around the crack. On fracturing at the interface the interface becomes stress free but this is achieved by a stress redistribution and decrease in the stress level. Table III shows the values of the residual shear stresses, σ_{xyres}, found by counting the number of fringes observed in the specimens.

TABLE III Residual stresses estimated from photoelasticity studies

Post-cure temp. (°C)	σ_{xyres}(initial) (MPa)	σ_{xyres}(final) (MPa)
20	0	0
45	0.35	0.10
80	0.65	0.25
120	1.65	0.45
150	1.65	0.80

Stress fringe value taken as 11.1 N mm^{-1} thickness per fringe.

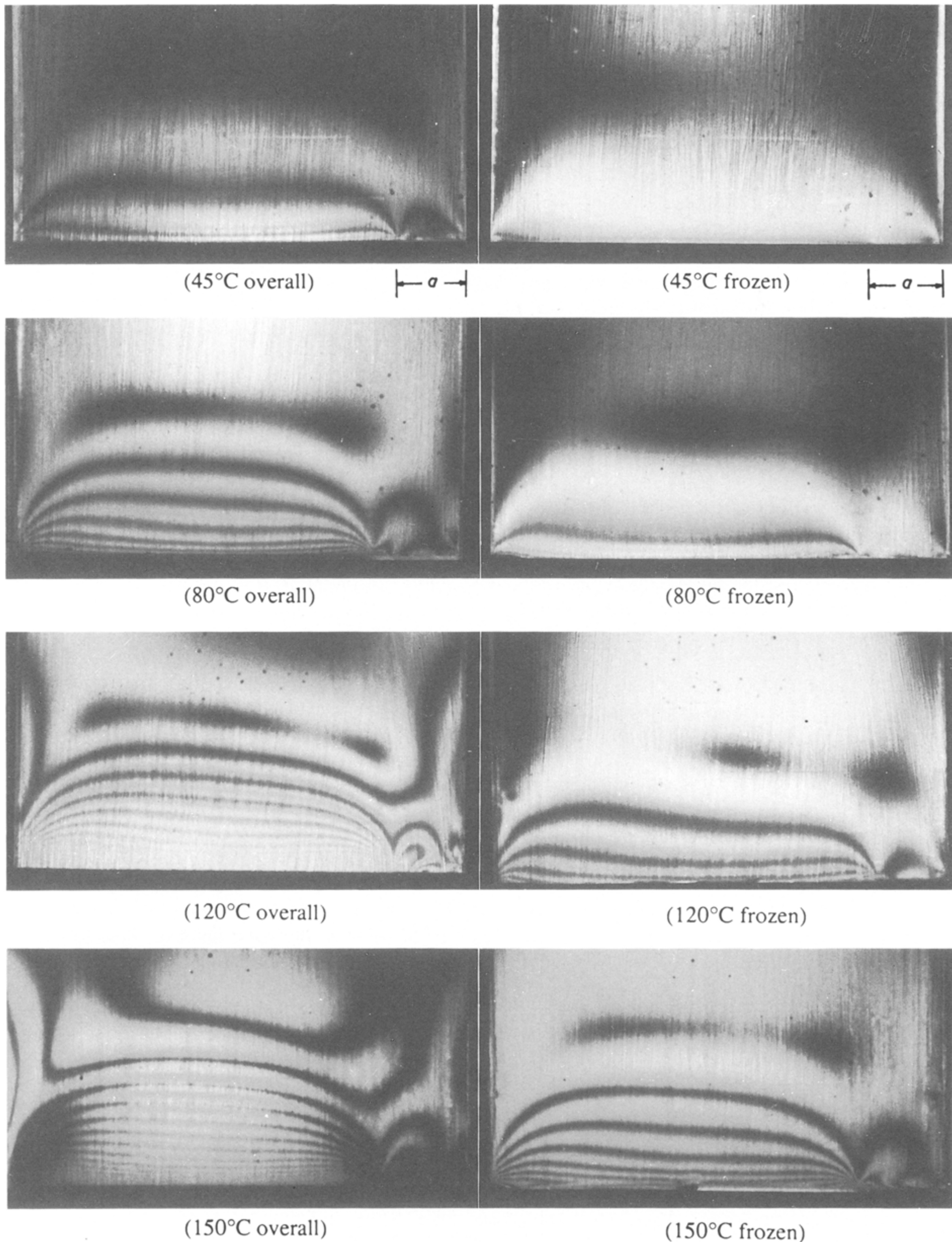

Figure 7 Isochromatic fringe patterns of residual stresses (a = 10 mm). The left-hand side series are for the adhesive layer in a SBM joint. The right-hand side series is taken after the adhesive layer has been debonded (interfacially) from the aluminium alloy substrate.

4.3.4. Superpositioning

It was not possible to pursue the direct photoelastic measurements in any detail because it proved too difficult to determine the stress intensity factors from the fringes. An approximation was therefore adopted in which the residual stresses were computed and a G_{res} was calculated and then added to the measured initiation value, G_{ic}, to give the effective value, G_{eff}, i.e.

$$G_{eff} = G_{ic} + G_{res} \tag{11}$$

This is effectively superimposing energies (or stresses squared) which is appropriate if the residual stresses were predominantly shear, thus giving an additional Mode II component. As discussed by Parker [24, 25],

it is necessary to superimpose stresses when the residual stresses are predominantly direct stresses. Thus, G_{eff} is proportional to $(\sigma_c^2 + \sigma_{res}^2)$ whilst superimposing stresses would give a term G'_{eff}, where G'_{eff} is proportional to $(\sigma_c + \sigma_{res})^2$ and hence

$$G'_{eff} = G_{eff} + 2G_{ic}\left(\frac{G_{eff}}{G_{ic}}\right)^{1/2} - 1 \quad (12)$$

No attempt was made to separate G_{res} into the mode components, so G_{eff} and G'_{eff} must be regarded as lower and upper bounds, respectively.

The first step towards evaluating the value of G_{res} was to ascertain the normal, σ_y, and shear, σ_{xy}, stresses along the interface for an uncracked SBM specimen. To accomplish the boundary integral equation (BIE) analysis was employed with a uniform stress boundary condition of $\sigma_x = -E\Delta\alpha\Delta T$ along the vertical edges of the epoxy adhesive. This is shown in Fig. 8 where $\Delta\alpha$ is the difference in the coefficients of thermal expansion and ΔT is the temperature difference between ambient (20 °C) and the post-cure temperature employed. Typical results are shown in Fig. 9 which reveal that both the direct and shear components are very high at the bond edge ($x/W = 0$) and the ratio of direct to shear components (normalized with respect to $E\Delta\alpha\Delta T$) at this point is about 3 in value. The residual direct stress falls sharply to a small compressive value at the middle of the plate along the interface ($x/W = 0.5$). The residual shear stress is, on the other hand, about the same value as the prescribed value of σ_x at the bond edge and reduces to zero at the middle of the plate. The normalized residual stresses for the SBM joint for each post-cure temperature exhibited very similar trends and this is not surprising because the differences in the properties of the epoxy adhesive as a function of post-cure temperature are small, see Table I. However, the absolute magnitudes of the residual stresses are quite large and increase, of course, with increasing temperature difference, ΔT. The average values of these shear stresses are about 1 MPa for a post-cure temperature of 45 °C rising to about 5 MPa for a post-cure temperature of 150 °C. These values are of the same order of magnitude as those deduced from using the photoelasticity results, see Table III.

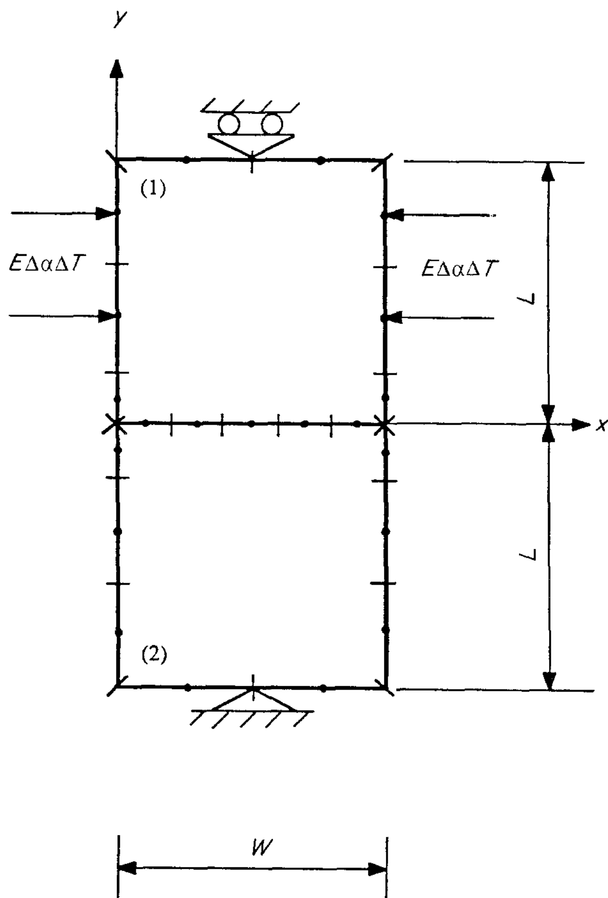

Figure 8 The mesh generated for the boundary integral equation (BIE) method of the SBM joint specimen when the adhesive layer is subjected to uniform compression.

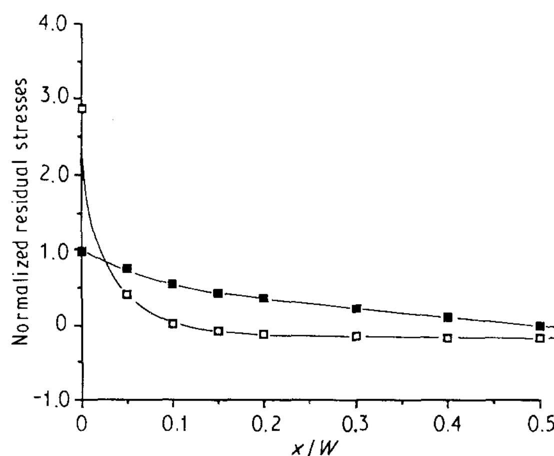

Figure 9 Residual stresses along the interface for the SBM specimen post-cured at 80 °C. The stresses were deduced using the BIE method and are normalized with respect to the applied stress, see Fig. 8. (□) σ_y, (■) σ_{xy}.

The value of G_{res} was estimated by means of the BIE method using the superposition principles of Parker. The stresses obtained from the above analysis, but with opposite signs, were prescribed as the boundary conditions over the crack faces. The J-integral values obtained from the BIE method directly gave the values of G_{res}. Various a/W ratios were considered and the results for G_{res} for post-cure temperatures of 120 and 150 °C are plotted against a/W ratios in Fig. 10. These results show that higher values of G_{res} occur at shorter crack lengths for all cases. This suggests that the importance of the residual stresses is more pronounced for the SBM specimens when they contain short cracks, especially for $a/W < 0.15$. Further, because the prescribed stresses consist of both normal and shear stresses, the G_{res} that is deduced is a mixed-mode fracture energy, i.e. both Mode I and Mode II components are involved. Because $\sigma_{xy} > \sigma_y$ (except near $a = 0$) it is likely that the true value of the interfacial fracture energy is closer to G_{eff} than to G'_{eff}.

4.3.5. Values of G_{eff} and G'_{eff}

A polynomial least squares curve-fitting technique was used to fit the results such as those shown in Fig. 10, so that relationships between G_{res} and a/W

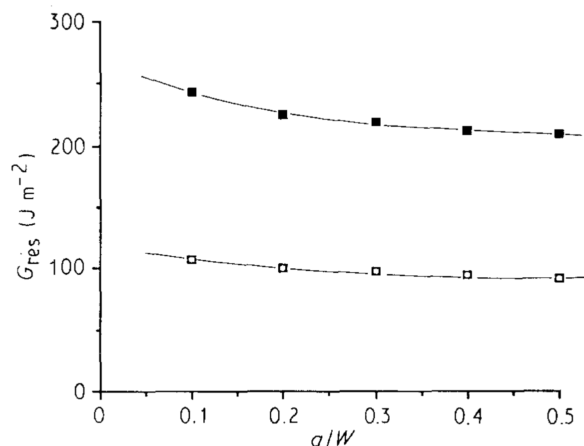

Figure 10 G_{res} plotted as a function of normalized crack length, a/W, for the SBM joint specimens which have been post-cured at (□) 120 and (■) 150 °C.

could be established. Subsequently, an effective adhesive fracture energy, G_{eff}, was deduced from Equation 11 by taking the appropriate values of G_{ic} and G_{res} for a given value of a/W for the post-cure temperature of interest. The values of G_{eff} so calculated are shown as a function of a/W in Fig. 11 for post-cure temperatures of 120 and 150 °C. It is evident that the values of G_{eff} are not a function of crack length. Thus, it appears that the dependence of the measured, or apparent, fracture energy, G_{ic}, on the value of a/W arises from the presence of the residual elastic stresses induced by differential thermal shrinkage; once these are accounted for the independence of the fracture energy upon initial crack length, as required by LEFM, is restored. The values of G'_{eff} were calculated using Fig. 12.

The values of G_{eff} and G'_{eff} are given in Table II and there are several points of interest. As commented above, the values of G_{ic}, G_{eff} and G'_{eff} are mixed-mode fracture energies because they consist of contributions from both Mode I and Mode II terms. However, as explained earlier, these terms do not have the clearly defined physical significance for the case of a crack at a bimaterial interface as for the bulk (homogeneous) material case. We have not attempted to separate the

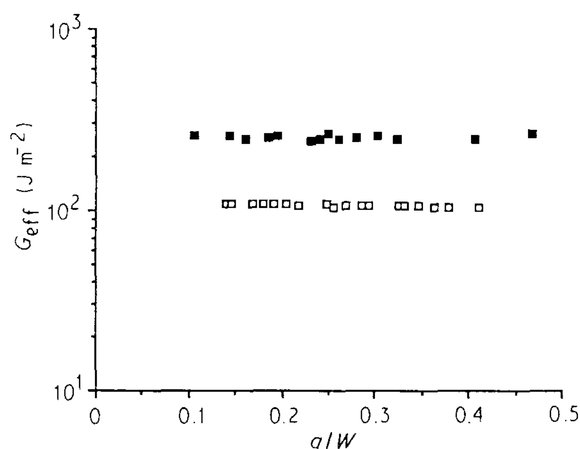

Figure 11 Values of G_{eff} plotted as a function of normalized crack length, a/W, for the SBM joint specimens which have been post-cured at (□) 120 and (■) 150 °C.

G values into the individual Mode I and II fracture energies. The computations of G_{eff} and G'_{eff} are approximate and ignore such factors as shrinkage and stress relaxation, so detailed quantitative deductions are probably not worthwhile. However, the magnitude of the computed stresses is known to be sensible from the photoelastic results (see Table III) and it is interesting to note that the value of G'_{eff} (deduced by summing stresses) is not greatly different from G_a or G_{Ic}. This is at first somewhat surprising because the fracture was apparently interfacial in many cases, as discussed below. However, it is of interest to note Bascom and co-workers [26, 27] have also reported that for brittle epoxy adhesives which possess low fracture energies, the value of the fracture energy for a crack running at, or close to, the epoxy/metal interface is similar in value to that for fracture of the bulk adhesive. Finally, of course, the values of G_{eff} and G'_{eff} are far greater than the corresponding measured values of G_{ic}. This emphasizes the importance of considering the contribution of residual stresses when deducing interfacial fracture energies.

4.3.6. Locus of failure

As explained above, in the SBM joint specimens which were post-cured at 20 °C the initial interfacial starter crack did not continue to propagate along the epoxy/aluminium interface but immediately diverted into the adhesive layer. In contrast, for the SBM specimens post-cured at 45, 80, 120 and 150 °C then the original interfacial starter crack did initially propagate along the interface. However, after propagating along the interface for some distance, the crack suddenly diverted into the adhesive layer and, thus, the final phase of joint fracture was again via cohesive failure in the adhesive. The higher the post-cure temperature, and higher the residual thermal stresses, the longer was the distance prior to the crack diverting into the adhesive layer.

5. Conclusions

Crack growth at a bimaterial interface has been studied by using symmetrical bimaterial (SBM) specimens which consisted of an epoxy adhesive bonded to an aluminium alloy substrate. The BIE method was found to model accurately the compliance of the SBM specimen containing an interfacial crack, and the general form of the LEFM equation (Equation 9) was employed to calculate the adhesive fracture energy, denoted by G_{ic}.

When the post-cure temperature used was ambient temperature (i.e 20 °C) the initial interfacial crack immediately diverted into the adhesive layer. In this case the value of G_{ic} was equivalent to the cohesive fracture energy, G_{Ic}, as determined from bulk single-edged notched (SEN) tests conducted on the epoxy adhesive. However, if elevated post-cure temperatures (i.e. temperatures of 45, 80, 120 and 150 °C) were employed then residual elastic stresses arising from differential thermal contraction of the adhesive and substrate

were found to influence both the manner in which the crack propagated and the measured value of G_{ic}.

Firstly, for the SBM specimens post-cured at 45, 80, 120 and 150 °C, the original interfacial starter crack did initially propagate along the interface. However, after propagating along the interface for some distance the crack suddenly diverted into the adhesive layer and, thus, the final phase of joint fracture was again via cohesive failure in the adhesive. The higher the post-cure temperature, and higher the residual thermal stresses, the longer was the distance prior to the crack diverting into the adhesive layer.

Secondly, a quantitative assessment of the influence of a residual stress field was made by proposing that an effective adhesive fracture energy could be defined whereby this term has contributions from both the residual and applied stress fields. The values of this parameter, G_{eff} and G'_{eff}, were considerably greater in value than the measured values of G_{ic}, clearly revealing the major contribution that arises from the residual elastic stresses to the failure process.

Acknowledgement
The authors thank Dr R. T. Fenner for his advice and assistance in running the BIE computations.

References
1. A. J. KINLOCH, "Adhesion and Adhesives: Science and Technology" (Chapman and Hall, London, 1987) p. 264.
2. S. S. WANG, J. F. MANDELL and F. J. McGARRY, *Int. J. Fract.* **14** (1978) 39.
3. A. J. KINLOCH and S. J. SHAW, *J. Adhesion* **12** (1981) 59.
4. M. L. WILLIAMS, *Bull. Seism. Soc. Amer.* **49** (1959) 199.
5. F. ERDOGAN, *J. Appl. Mech.* **30** (1963) 232.
6. J. R. RICE and G. C. SIH, *ibid.* **31** (1964) 477.
7. *Idem., ibid.* **32** (1965) 418.
8. B. M. MALYSHEV and R. L. SALGANIK, *Int. J. Fract. Mech.* **1** (1966) 114.
9. J. G. WILLIAMS, "Fracture Mechanics of Polymers" (Ellis Horwood, Chichester, 1984) p. 55.
10. A. J. KINLOCH (ed.), "Durability of Structural Adhesives" (Applied Science, London, 1983).
11. A. A. GRIFFITH, *Phil. Trans Roy. Soc.* **A221** (1920) 163.
12. E. OROWAN, *Rep. Prog. Phys.* **12** (1948) 185.
13. G. R. IRWIN, *Appl. Mater. Res.* **3** (1973) 65.
14. H. M. WESTERGAARD, *J. Appl. Mech. A* June **6** (1939) 46.
15. B. GROSS, J. E. SRAWLEY and W. F. BROWN, NASA Report TN D-2395 (1964).
16. S. MOSTOVOY, P. B. CROSLEY and E. J. RIPLING, *J. Mater.* **2** (1967) 661.
17. S. MOSTOVOY and E. J. RIPLING, *J. Appl. Polym. Sci.* **10** (1966) 1352.
18. S. MOSTOVOY, P. B. CROSLEY and E. J. RIPLING, *Engng Fract. Mech.* **3** (1971) 421.
19. G. KARAMI, PhD Thesis, University of London (1983).
20. G. KARAMI and R. T. FENNER, *Int. J. Fract.* **30** (1986) 13.
21. J. MIJOVIC and J. A. KOUTSKY, *Polymer* **20** (1979) 1095.
22. S. S. LABANA, S. NEWMAN and A. J. CHOMPFF, "Polymer Networks", edited by A. J. Chompff and S. Newman (Plenum Press, New York, 1971) p. 453.
23. D. R. MULVILLE and R. N. VAISHNAV, *J. Adhesion* **7** (1975) 215.
24. A. P. PARKER, ASTM STP 776 (American Society for Testing and Materials, Philadelphia, PA, 1982) p. 13.
25. *Idem., J. Mech. Working Tech.* **10** (1984) 165.
26. W. D. BASCOM, C. O. TIMMONS and R. L. JONES, *J. Mater. Sci.* **10** (1975) 1037.
27. W. D. BASCOM and J. OROSHNIK, *J. Mater. Sci.* **13** (1978) 1411.

Received 30 October
and accepted 19 November 1990